Int. J. Electrochem. Sci., 17 **(2022)** Article Number: 221021, doi: 10.20964/2022.10.06

International Journal of
ELECTROCHEMICAL
SCIENCE
www.electrochemsci.org

Study on the effect of electrokinetic methods combined with and solidification/stabilization technique for remediation of Cu2+-contaminated soil under different voltage gradients

Wang Wen[1], Lijun Jia[2], Wenjing Zhao[2], Huimin Feng[2], Dehua Cao[2], Jun Xie[1],Tingfei Xu[1], Mingye Cui[1], Wenting Zhou[1], Qian Mei[1], Pengju Han[1], Xiaohong Bai[1], Bin He[1,]*

[1] College of Civil Engineering, Taiyuan University of Technology, Taiyuan, 030024, China
[2] Shanxi Shan'an Lide Environmental Science &Technology Co., Ltd, Taiyuan, 030032, China
[*]E-mail: hebin@tyut.edu.cn

Received: 27 June 2022 / *Accepted:* 9 August 2022 / *Published:* 10 September 2022

In this paper, contaminated kaolin soil containing copper ions was remediated using the electrokinetic (EK) method combined with a solidification/stabilization (S/S) remediation technique by applying different voltages. The electric current changes during remediation, soil moisture contents, soil pH, soil electrical conductivity (EC) in each area before and after remediation, changes in copper content of the soil before and after remediation, and energy consumption analysis were systematically studied to evaluate the remediation effect on the contaminated soil. The results showed that, when 30 V was applied, the removal efficiency of the EK-S/S combined remediation technique was 66.51%, which was 20% higher than the EK remediation efficiency, and the energy consumption was only 14.62 kWh/m^3. The solidifying agent in the region near the cathode (S1) can effectively solidify the copper ions migrating to this location. It had a high EC, which is conducive to the migration and fixation of metal ions, and its pH was between 11-12, which means it is an environmentally friendly solidifying agent that does not cause harm to the environment. After the leaching toxicity test, the Cu^{2+} concentration of the solidifiers was approximately 20 mg/kg, and, as the remediation time increased, the more fully it reacted internally, improving its solidifying effect.

Keywords: Combined remediation technology; Voltage gradient; Cu^{2+}-contaminated kaolin; Energy consumption analysis.

1. INTRODUCTION

With the continuous development of the economy, soil heavy metal pollution, with pollutants such as Cu, Zn, Pb, As, Ge, Hg, and Ni, has become increasingly severe. It has become one of the major environmental problems in China[1,2]. The types of soil pollution in China are diversified, and the

pollution sites are complex, including farmland, mines and construction sites. These heavy metals will eventually enter the human body through various channels, which will cause great harm to human health[3,4]. In response to heavy metal contamination pollution, many researchers have developed a series of remediation technologies for purifying soil, such as solidification/stabilization (S/S) techniques, soil flushing techniques, electrokinetic (EK) remediation techniques, bioremediation techniques, and combined remediation techniques[5-9]. Among them, the S/S remediation technique is the most widely used, but the single use of this technique requires a large number of solidifiers and water resources. It is easy to cause extensive soil disturbance and only changes the fugitive form of heavy metals without fundamentally removing them[10]. The EK remediation technique is also a promising technology that is suitable for the remediation of high-moisture content, dense and low permeability soils with organic–inorganic composite contamination[11]. EK remediation of heavy metal soils mainly relies on electromigration and electroosmosis under a direct current (DC) electric field to concentrate heavy metals and minerals in the soil in a fixed location, and then centralized treatment is applied. However, the traditional single EK remediation technique has problems such as high cost, tendency to cause secondary pollution of water resources, the need for secondary treatment of its electrolyte, and difficulty in promotion. The high cost of EK remediation is the main obstacle to its widespread application[12]. The specific costs mainly include the fabrication and assembly of electrode materials, labour, electrical energy consumption[13,14], and secondary treatment of electrolytes and soil at the location of heavy metal accumulation[15].

The starting point of this research is to overcome the shortcomings of the EK remediation techniques and the S/S remediation techniques and to combine them (EK-S/S combined remediation techniques). Specifically, a solid waste solidifying agent synthesized from red mud (RM) and fly ash (FA) as the main raw materials combined with a small amount of high belite sulfoaluminate cement (HBSC) and quicklime is placed in the area near the cathode during the EK remediation process. Under the action of the electromotive force, the copper ions will migrate to the region near the cathode, where the solidifier will effectively cure them.

In particular, different voltage strengths have an effect on the migration of copper ions, the electrodialysis rate, and the loss of electrode material during the EK remediation process. Chio et al.[16] systematically studied the electrical conductivity (EC) electrodialysis flow rate, pH, and phosphate migration changes in agricultural soils by setting a voltage gradient of 0.5 V/cm, 1.0 V/cm, and 2.0 V/cm. The results showed that, under electric field conditions of 0.5 V/cm and 1.0 V/cm, the soil EC and the pH of the cathode and anode had no obvious changes, and the electrodialysis flow rate and removal efficiency were also much lower than 2.0 V/cm. Torabi et al.[17] used an electrokinetic method to remove Cd and Cu from the contaminated soil of the Koushk mine tailings dam. Comparing two voltage gradients of 1 V/cm and 2 V/cm showed that higher voltages favoured the removal of heavy metals. Cang et al.[18] studied the effect of different voltage gradients on the uptake of heavy metals Cd, Cu, Pb, and Zn by mustard, applying 0 V/cm, 1.0 V/cm, 2.0 V/cm, and 4.0 V/cm of DC voltage for 8 hours per day for 16 days. The results showed that the applied electric field could promote the uptake of metals by plants, and the voltage gradient of 2.0 V/cm had the highest plant metal accumulation. Therefore, it is necessary to study the remediation effect of EK-S/S combined remediation techniques at different voltage intensities.

In this study, 4 voltage gradients were set up to systematically study various parameters, including electric current changes, changes in soil moisture contents, pH, EC, and Cu^{2+} content in the soil. Combined with energy consumption analysis and remediation efficiency calculations, we used this data to determine the optimal value of the DC voltage applied for the EK-S/S combined remediation techniques.

2. EXPERIMENTAL

2.1. Experimental materials

The soil samples were taken from kaolin produced by the Henan platinum run. The samples are composed of a single component, and such soil is widely distributed in China, convenient for experimental research. The chemical composition of kaolin is listed in Table 1. The particle size was measured by a BT-9300S laser particle size analyser. As shown in Figure 1, the sizes of D10, D50, and D90 of kaolin were estimated to be 1.343 μm, 14.02 μm, and 42.52 μm, respectively. This means that particles smaller than 42.52 μm accounted for 90% of the sample, and the specific surface area was measured as 580.3 m^2/kg. The mineralogical phases of kaolin were also tested by XRD. As depicted in Figure 2(a), the main mineralogical components of kaolin were cristobalite (SiO_2) and mullite ($Al_6Si_2O_{13}$).

The RM used in this study was selected from the Bayer method RM produced by an aluminium plant in Wenshui of the Shanxi province of P.R. China. As illustrated in Table 1, the main chemical composition included SiO_2, Al_2O_3, and CaO. The raw material was sieved through a 0.5 mm screen after drying and crushing. According to the particle size distribution in Figure 1, the specific surface area was estimated to be 1079 m^2/kg. In addition, the mineralogical phases of RM were tested by XRD, and the data showed that RM was mainly composed of gibbsite [$Al(OH)_3$], katoite [$Ca_3Al_2SiO_4(OH)_8$], calcite ($CaCO_3$), and cancrinite [$Na_6Ca_2Al_6Si_6O_{24}(CO_3)_2 \cdot 2H_2O$] (Figure 2(b)). FA was obtained from Gongyi Longze Water Purification Material Co., Ltd. of P.R. China. The grade consisted of secondary ash with the main chemical composition of SiO_2 and Al_2O_3. The particle size distribution is shown in Figure 1. The specific surface area was estimated to be 489.4 m^2/kg. The mineralogical phases of FA were tested by XRD, and the data are summarized in Figure 2(c). FA was mainly composed of SiO_2, mullite ($Al_6Si_2O_{13}$), haematite (Fe_2O_3), and calcite ($CaCO_3$).

HBSC was supplied by the Polar Bear Cement Plant in Tangshan, Hebei Province of P.R. China. The strength grade of the cement was 42.5 grade. The particle size distributions of HBSC are shown in Figure 1. The specific surface areas of both materials were estimated to be 438.5 m^2/kg and 590.1 m^2/kg, respectively. The main chemical composition is shown in Table 1. The XRD results also showed that the main mineralogical components of HBSC were of $CaSO_4$, C_2S, and $C_4A_3\bar{S}$ (Figure 2(e)).

The quicklime was used in combination with analytically pure CaO produced by Tianjin Tianli Chemical Reagent Co., Ltd. The copper-based ions employed for testing were analytically pure $Cu(NO_3)_2 \cdot 3H_2O$ produced by Founder's Reagent Factory in Beichen, Tianjin. All chemicals used in the experiments were of analytical grade, and distilled water was used throughout testing.

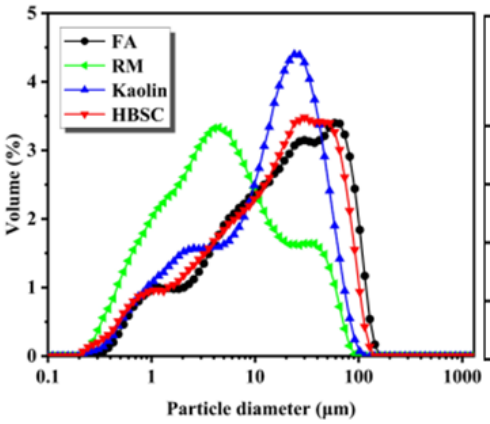

Material	D10(μm)	D50(μm)	D90(μm)	Specific surface (m^2/kg)
Kaolin	1.343	14.02	42.52	580.3
RM	0.763	4.265	29.92	1079
FA	1.584	17.24	70.79	489.4
HBSC	1.34	15.76	60.25	590.1

Figure 1. The particle size distribution of materials.

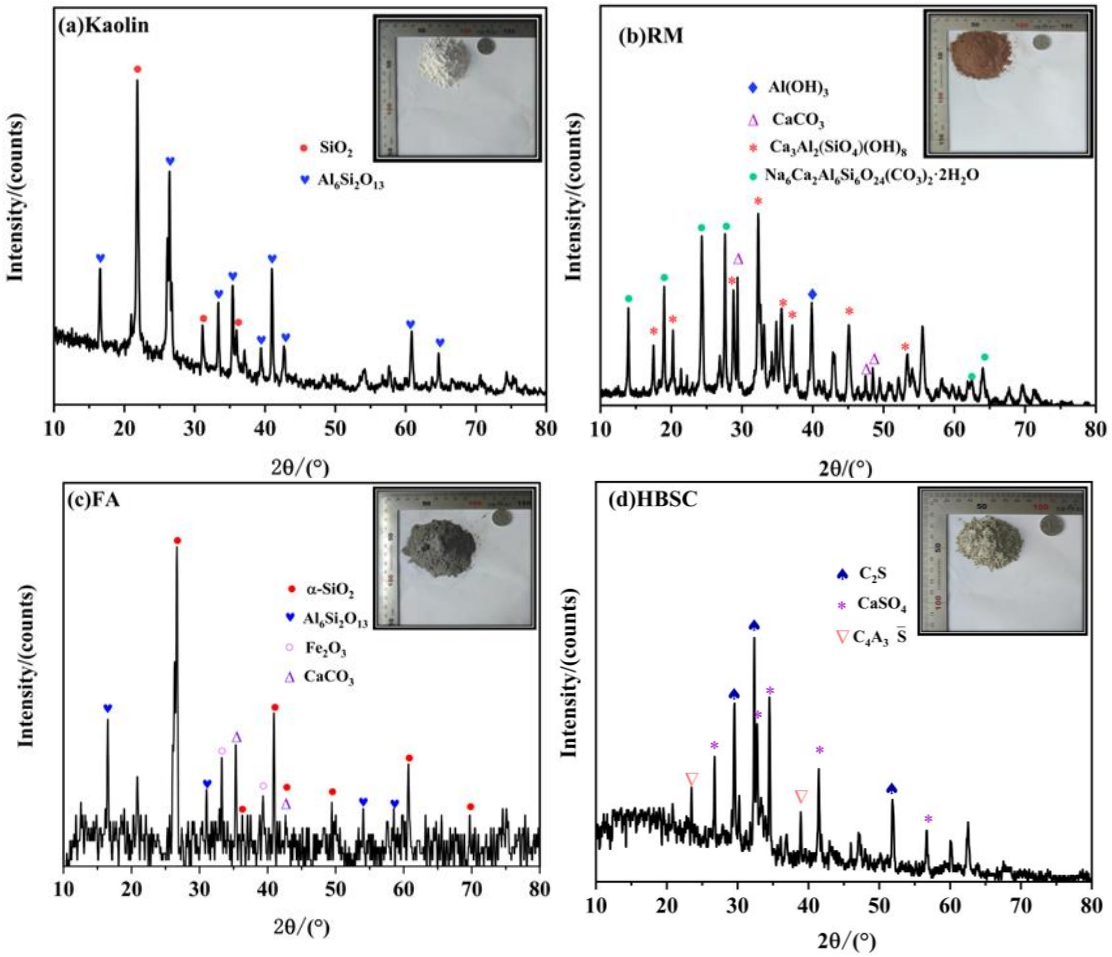

Figure 2. X-ray diffractograms of(a) kaolin, (b) RM, (c) FA , and (d) HBSC.

Table 1. The main chemical composition of test materials.

	Chemical composition (%)									
	Al_2O_3	SiO_2	Fe_2O_3	CaO	MgO	K_2O	TiO_2	Na_2O	SO_3	LOSS
Kaolin	44.42	52.68	0.48	0.24	0.17	1.11	44.42	-	-	0.9
RM	22.72	21.43	9.98	16.49	-	0.42	3.98	11.51	-	13.41
FA	31.15	53.97	4.16	4.01	1.01	2.04	-	0.89	0.727	-
HBSC	18.59	13.98	2.02	50.74	2.15	0.21	-	-	11.75	-

2.2. Cu^{2+}-contaminated soil and solidifying agent

In this experiment, commercial kaolin clay was used as a soil model. $Cu(NO_3)_2 \cdot 3H_2O$ (analytical grade) was used to configure the Cu^{2+} contamination solution to a pH of 4.26. The kaolin and the contamination solution were thoroughly mixed using a mortar mixer and loaded into an electrolytic cell (as shown in Figure 3). The physical and chemical properties of the soil and solidifiers are shown in Table 2. The solidifying agent used in the experiment was the low-energy HBSC synergistic solid waste solidifier previously developed by our research group. The solidifier consists of RM and FA, the total amount of which is 35%; the red mud-fly ash ratio is 8:2 and the water-cement ratio is 0.45 with 7% HBSC and 3.5% quicklime.

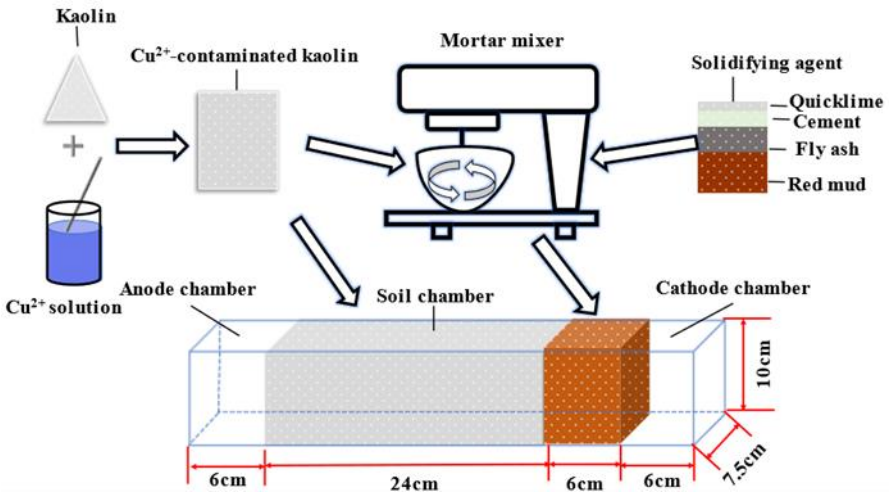

Figure 3. Loading of Cu^{2+}-contaminated soil and soil solidifying agent into a plexiglass tank.

Table 2. Physical and chemical properties of the soil and Solidifying agent

	Moisture content (%)	pH	EC (μs/cm)	Cu^{2+} (mg/kg)
Clean soil	0.02	6.75	213	0
Contaminated soil	45	5.32	348	398
Solidifying agent	45	11.46	1612	398

2.3. Test Instruments and Equipment

The main instruments and equipment used in the test were a GPC-H linear DC power supply (Guwei Electronics Industrial Co., Ltd., China), mixer barrel and blade, FE28 benchtop pH metre (Mettler-Toledo Instruments (Shanghai) Co., Ltd., China), inductively coupled plasma spectrometer (SPECTRO ARCOS, Germany), Raycom DDS-307A EC metre (Shanghai Yidian Science Instruments Co. Ltd., China), BT100-12 constant flow pump (Shanghai Qingpu Huxi Instrument Factory, China), THM industrial paperless recorder (Fai Control Co., Ltd., China), electric centrifuge, YKZ-08 flip-type oscillator, and horizontal oscillator. As shown in Figure 4, the EK remediation device is a self-designed Plexiglas tank, including a soil chamber (30 cm×7.5 cm×10 cm) with two porous partitions on both sides of the electrolysis tank separating the soil chamber from the electrode chambers. The partitions are wrapped with qualitative filter paper to prevent soil particles from entering the electrode chambers. The soil was divided into five equal parts in the cathode to anode and numbered S1 to S5 to facilitate sampling studies.

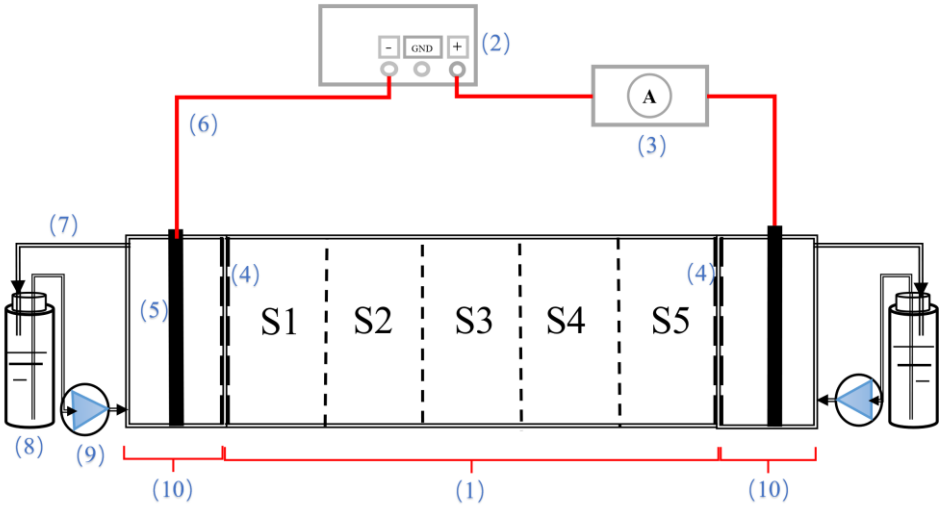

Figure 4. A schematic view of the electrokinetic laboratory setup: (1) Soil chamber, length: 30 cm, width: 7.6 cm, height: 10 cm. (2) DC power supply. (3) Current recorder. (4)Porous glass plate and filter paper. (5) Electrode plate. (6) Lead wire. (7) Hose. (8) Wide mouth bottle (provides electrolyte). (9) Peristaltic pump. (10) Electrolyte reservoirs.

2.4. Experimental process

The S1 area of the electrolysis tank was filled with a solidifying agent with a mass ratio of 8:2 of

RM and FA and Cu^{2+}-contaminated kaolin soil mixed thoroughly. The S2-S5 area was filled with Cu^{2+}-contaminated kaolin soil (as shown in Figure 5(a)). Distilled water was used as the electrolyte in both electrode chambers. Two-litre Teflon bottles were filled with 1.5 L of distilled water. The water was introduced into the electrode chambers at a rate of 30 ml/min through a constant flow pump. Holes were opened in the outer wall of the electrode chamber where the soil height was level, and the electrolyte in the electrode chamber circulated into the bottles when it reached a certain height, equilibrated for a while and connected to the power supply. After balancing for a period of time and connecting to the power supply, the remediation time is 72 hours, and the voltage gradients are set to 0.5 V/cm, 1 V/cm, 1.5 V/cm, and 2 V/cm; 15 V, 30 V, 45 V, and 60 V are applied. A control group was also established with a voltage gradient of 1 V/cm (*30 V), and all contaminated soils were placed in the soil chamber area S1-S5 (as shown in Figure 5(b)), while other conditions were kept the same. During the remediation process, a paperless recorder was used to record the primary electric current for half an hour. Measurements of pH, EC, and copper ions in soil and electrolyte and the moisture contents of the soil were taken at the end of the experiment.

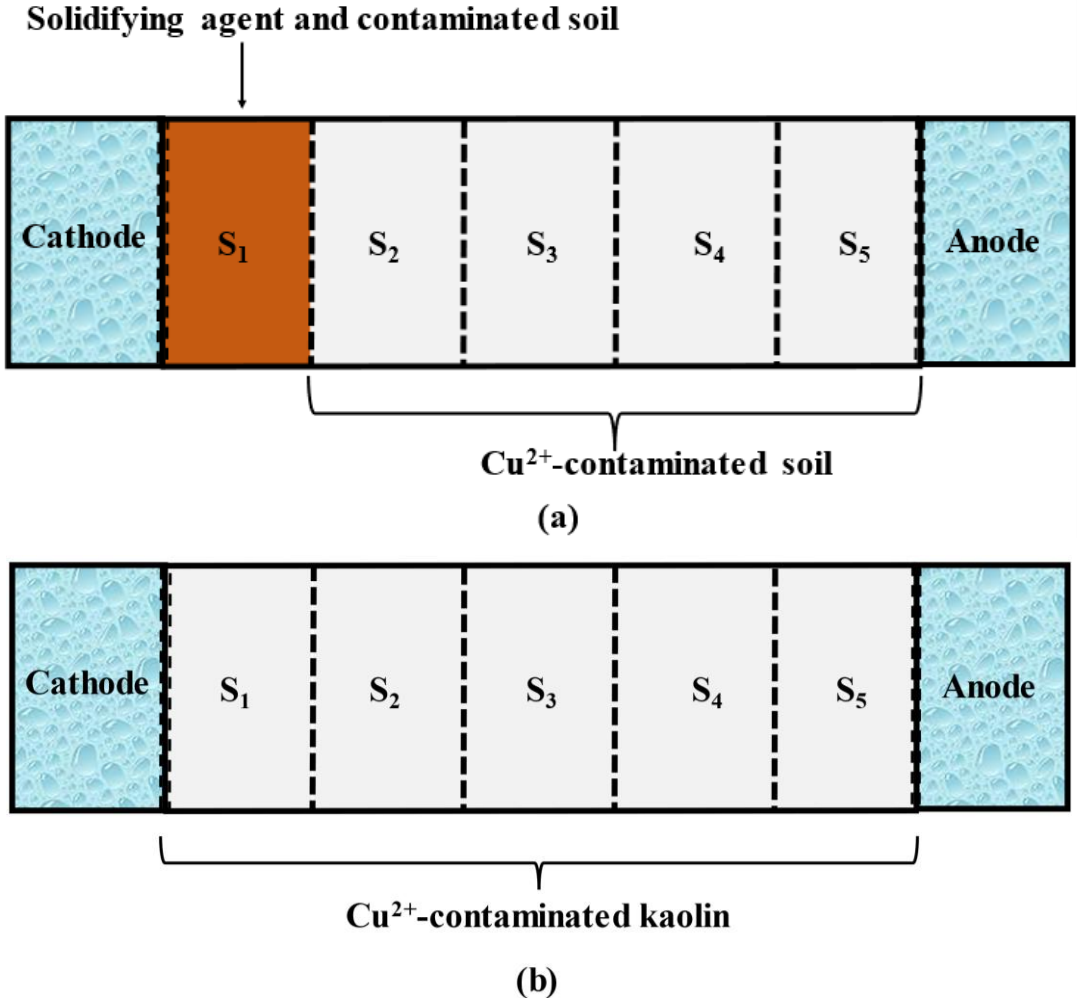

Figure 5. Experimental diagrams: (a) Combined remediation; (b) EK remediation.

2.5. Analysis methods

2.5.1. Moisture contents of the soil and solidifying agent

The aluminium box was first weighed (m_1) and numbered. After the remediation was completed, the soil samples of each area were removed, placed in an aluminium box and weighed (m_2). Three parallel samples were set in each area and then dried in an oven, removed, and allowed to cool; finally, the samples were weighed (m_3). The moisture content was calculated according to Equation 1.

$$\omega = \frac{m_2 - m_3}{m_3 - m1} \times 100\% \quad (1)$$

Where ω is the moisture content (%), m_1 is the weight of the aluminum box (kg), m_2 is the weight of the aluminum box humidified soil (kg), and m_3 is the weight of the aluminum box plus dry soil (kg).

2.5.2. Soil pH

The weighed 10.00 g air-dried soil samples were placed in a 50 mL polypropylene centrifuge tube, 25.00 mL of deionized water was added, then the bottle was sealed and placed it in a horizontal shaker for vigorous shaking for 2 min. The pH of the supernatant was determined by inserting the electrode into the solution[19].

2.5.3. Electrolyte pH

Twenty millilitres of electrolyte was placed in a 50 mL centrifuge tube and allowed to stand for 30 min. The pH metre electrode was inserted into the solution, and the pH value of the supernatant was measured.

2.5.4. EC of soils and solidifiers

After the soil samples were removed, they were air-dried, subdivided, ground, and passed through a 2 mm sample sieve. A 5.00 g soil sample and 25 mL of deionized water were placed in a 50 mL polypropylene centrifuge tube. The tube was placed in a duplex horizontal constant temperature oscillator and shaken at 20±1 °C for 30 min. After fully mixing the soil and water, the mixture was allowed to stand for 30 min and filtered with qualitative filter paper. The filtrate was collected in a 100 mL beaker and measured by an EC metre[20].

2.5.5. Soil Cu^{2+} concentrations

A total of 3.0 g of air-dried contaminated soil was added to a 50 mL centrifuge tube containing 30 mL of 1 mol/L HCl, shaken at 200 rpm for 6 h, and centrifuged at 4000 rpm for 15 min[21]. The concentrations of copper ions in the supernatant were filtered through a 0.22 mm filter and measured by inductively coupled plasma–optical emission spectrometry (ICP–OES).

2.5.6. Cu^{2+} concentrations in catholyte

A total of 20 mL of electrolyte was placed in a 50 mL centrifuge tube, and 1-2 drops of dilute nitric acid were added dropwise. The tube was shaken well to reduce the pH, filtered, and measured by ICP–OES.

2.5.7. Toxic leaching tests

The leaching toxicity was tested since the solid waste sufficiently mixed and reacted with the Cu^{2+}-contaminated soil. According to the Chinese standard[22], the following steps were specifically tested.

1) The moisture content of the solidified soils was determined. To this end, a 50-100 g sample was then weighed in a covered container, dried at 105 ° C, repeatedly weighed until the error of two weighing values became less than ±1%, and finally tested for the water content.

2) The leaching agent was prepared by adding a mixture of concentrated sulfuric acid and concentrated nitric acid at a mass ratio of 2:1 to distilled water (approximately 2 drops of the mixture in 1 L of water). The pH of the prepared leaching agent was fixed at approximately 3.2±0.05.

3) The volumes of the leaching agent and mass of the cured soil sample were calculated according to the moisture content of the sample at a liquid to solid ratio of 10:1 (L/kg). Both were then loaded into 2 L Teflon bottles.

4) The bottle on the YKZ-08 tilting oscillator was fixed, the rotation speed was adjusted to 30±2 r/min, and the vibration was set to 23±2 °C for 18±2 h.

5) The bottles were removed and left to stand, the supernatant was collected by filtration, and the Cu^{2+} concentration was measured using a Spectrol Arcos ICP–OES instrument.

2.5.8. pH of solidifiers

According to the Chinese standard[23], the following steps were specifically tested.

1) The solidifying agent was dried and passed through a 5 mm sieve. Then, 100 g of sample was weighed and placed in a polyethylene bottle containing 1 L distilled water and sealed with the bottle cap.

2) Polyethylene bottles were vertically fixed on the horizontal oscillation instrument (the oscillation frequency was 110±10 times/min, amplitude was 40 mm, temperature was 23 ° C),oscillated for 8 h, then left standing for 16 h.

3) The samples were filtered with filter paper, and the supernatant was collected and measured with a pH metre.

2.5.9. power consumption

Equation 2 was used for electrical energy consumption analysis[24].

$$E = \frac{1}{V_s}\int VIdt \quad (2)$$

Where E is the electrical energy per unit volume (kWh/m^3), I is the applied electric current (mA), V is the voltage (V), t is the remediation time (h), and Vs is the soil volume (m^3).

3. RESULTS AND DISCUSSION

3.1. Changes in current during processing

The electric current changes over time during the remediation process are shown in Figure 6, showing that the electric currents of 15 V, 30 V, 45 V, and 60 V with different voltage gradients and 30 V in the control group increased to the peak first, then decreased continuously, and finally stabilized at 2.6 mA, 6.8 mA, 5.6 mA, 7 mA, and 1.5 mA, respectively. After treatment for approximately 50 h, the electric current tends to be stable. With the increase in voltage, the corresponding peak value also increased; the electric current of the control group after stabilization was lower than that of the other four groups.

The electric current increases first mainly due to the initial phase of energization, the time required for the electrodes to fully react, and the presence of numerous mobile ions in the soil chamber, to which the electric current is proportional[25]; therefore, the electric current starts with an increasing trend. As the remediation process proceeds, the migrating OH^- generated by the cathode enters the soil, and the solidifying agent combines with Cu^{2+} to form a nonmigratory precipitate[26]. The solidifying agent near the cathode undergoes a hydration reaction to form a gelling-like substance that traps and adsorbs copper ions, increasing the resistance of the soil chamber and reducing the number of mobile ions in the soil chamber, thus reducing the electric current in the remediation process. The resistance of the soil is fixed when it starts to be energized, and, according to Ohm's law, when the resistance is certain, the higher the voltage is, the higher its electric current. Therefore, the voltage gradient of 2 V/cm in this test has the highest peak. After 50 hours of remediation, the electric current eventually stabilize within a certain range due to the continuous migration of the dissolved state ions in the soil chamber under the action of the electric field, and the two form a dynamic equilibrium.

During the test, a large number of bubbles were observed covering the surface of the electrode plate, which may also be the reason for the low electric current at the latest stage of remediation. $Cu(OH)_2$ precipitation in the cathode chamber of the control group also affects the operation of the electrode to some extent.

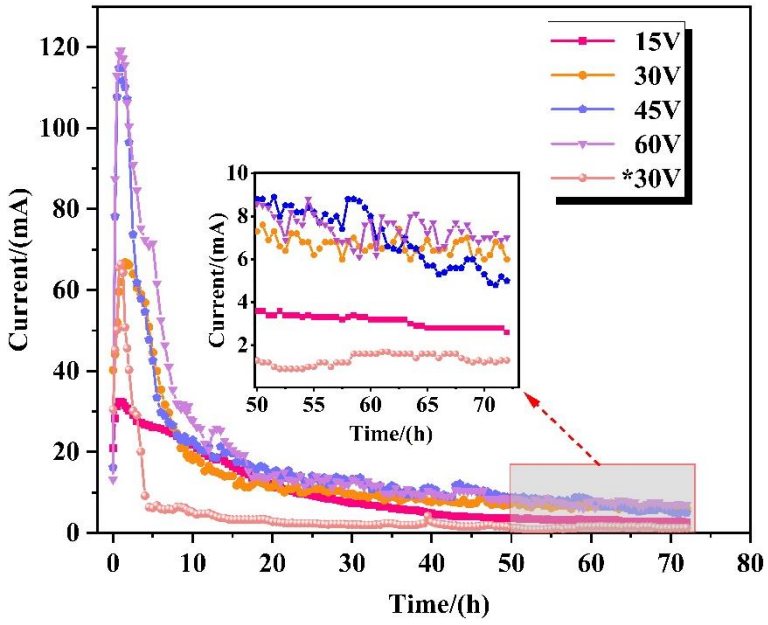

Figure 6. Changes in electric current with time under different voltage.

3.2. Soil moisture content

The changes in soil moisture contents in the soil chamber after the completion of the remediation test are shown in Figure 7, showing that the soil moisture contents in the S3 area in the middle part of the soil chamber are higher than those in both sides, the soil moisture contents in the S1 area near the cathode area are higher than those in the S5 area near the anode area, and the soil moisture contents decrease as the voltage increases. The moisture contents of the soil in the control group are high, at an initial soil moisture content of approximately 45%. The moisture contents of the soil in the area near the two poles are not very different.

The moisture contents of the soil in the middle region are higher than those on both sides, probably due to the migration of H^+ produced by the anode and OH^- produced by the cathode meeting in the soil to form water molecules, resulting in a high moisture content of the soil in the soil chamber. The ionic mobility of H^+ is 3625×10^{-6} $cm^2/(V\cdot s)$, while the ionic mobility of OH^- is 2058×10^{-6} $cm^2/(V\cdot s)$, and the migration rate of hydrogen ions is 1.8 times higher than that of hydroxide ions[27], so the moisture contents in the S2-S4 regions are generally higher. The solidifying agent in the S1 region consumes some water during the hydration reaction. Since the test time is not very long, there are still large pores inside the solidifying body, which do not cause pore blockage while fixing copper and have little effect on the electroosmotic water flow from the anode to the cathode; therefore, the moisture contents of the soil in the S1 region are higher than those in the S5 region. The larger the voltage is, the more rapid the electrode reaction, and the faster the speed of electroosmotic water flow is, the lower the soil moisture content is.

The control group belongs to the fully EK remediation process, during which Cu^{2+} precipitates near the cathode because of alkalinity, and there is an aggregation effect which impedes the electroosmotic water flow to a certain extent.

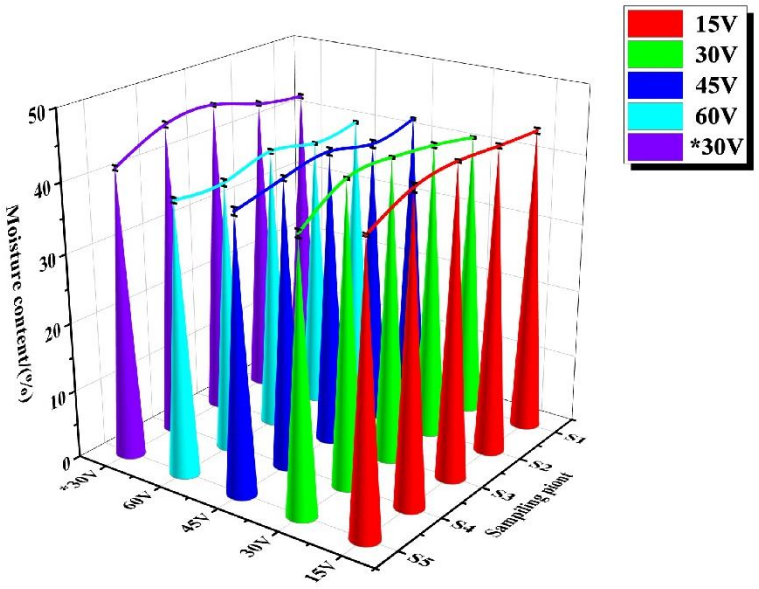

Figure 7. Changes in soil moisture contents at different locations under different voltage gradients.

3.3. Soil pH after treatment

The pH of the soil is an important factor affecting the removal of copper ions from the soil, and a lower pH promotes the dissolution of copper ions in soil and facilitates their removal by electrodialysis and electromigration[28]. The pH values of the soil, solidifying agent, and electrolyte before treatment were 5.32, 11.46, and 7.01, respectively. After the remediation was completed, the pH of the soil in the soil chamber is shown in Figure 8. During the combined remediation experiment, the electrode reaction occurred in the electrode plate, and the oxidation reaction in the anode chamber produced H^+, resulting in the pH of the anode electrolyte decreasing to between 1.5 and 2.2; the reduction reaction in the cathode chamber produced OH^-, resulting in the pH of the cathode electrolyte increasing to approximately 11. The S1 area was loaded with the solidifying agent, and the pH was high and stable between 11-12 under different remediation voltage conditions. The main reasons are that the OH^- generated by the cathode migrates into the soil under DC voltage, and the materials that make up the solidifying agent undergo a series of chemical reactions with their own high pH values. The pH changes in the S2-S5 regions are large, and the pH of the soil gradually decreases from the anode to the cathode. This is mainly due to the migration of H^+ generated in the anode chamber to the soil through electromigration and electroosmotic flow, resulting in a decrease in pH in the soil region near the anode[29]; conversely, the migration of OH^- generated in the cathode chamber leads to an increase in pH in the soil region near the cathode[30].

The pH of the soil in the control group showed a decreasing trend from the anode to the cathode, but the change was not large and close to the pH of the initial contaminated soil, probably because the electric current was small, the electrolysis reaction was not very violent and the ion migration rate was not too fast; therefore, the pH did not change much.

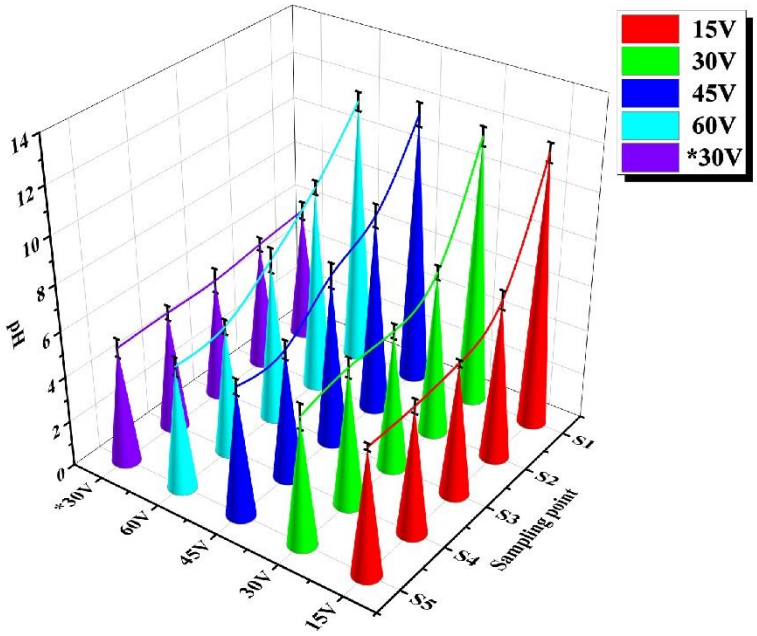

Figure 8. Changes in soil pH at different locations under different voltage gradients.

3.4. Soil EC after treatment

Soil EC can significantly affect the efficiency of EK remediation. Typically, a higher soil EC means a higher number of ions that can migrate in the soil and thus a shorter time spent on the EK remediation processes[31]. The changes in soil EC in the soil chamber after the remediation was completed are shown in Figure 9. In general, the higher the voltage in the same area is, the smaller the EC during the combined remediation. This may be because the higher the voltage intensity is, the more actively the soil ions migrate and the more they migrate to the electrode chamber, i.e., the fewer mobile ions are present in the soil. Specifically, the S1 region is a solidifier, and its EC is high at approximately 1600 $\mu s \cdot cm^{-1}$, which is mainly because the solidifying agent itself has a high EC and cation migration to the S1 region is high. In the S2-S5 regions, EC performance from S5 (near the anode) to S2 soils EC gradually decreased, which may be due to the role of electric current and electroosmotic flow along with cation migration from the anode to the cathode. The EC of the soil in the area near the anode is close to the initial EC of the contaminated soil, which indicates that the ions in this area maintain a dynamic balance of migration in and out of the region.

The EC of the control group was lower, and the soil EC tended to decrease from the anode to the cathode, mainly because the aggregation effect tended to occur near the cathode during the remediation process, and the EC of the migratory ions decreased, while the anode maintained a dynamic equilibrium near the initial EC of the contaminated soil.

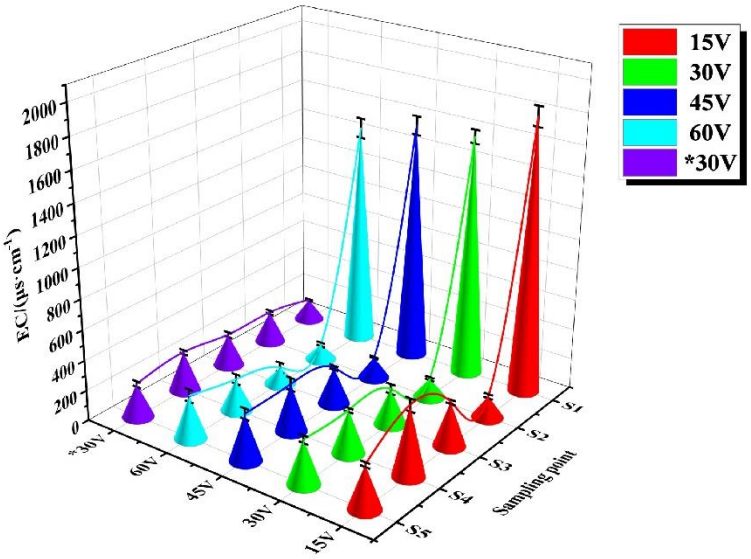

Figure 9. Changes in soil EC at different locations under different voltage gradients.

3.5. Changes in soil Cu^{2+} concentrations after remediation treatment

The residues of Cu^{2+} in each region of the soil chamber after the remediation treatment and the toxic leaching concentrations in the S1 region in the combined remediation experiment are shown in Figure 10. Under DC voltage, copper ions in soil are mainly transported to the cathode by electromigration, electroosmotic flow, and diffusion[32].

As shown in Figure 10, after the EK remediation treatment, the copper ion contents of the soil at all locations were lower than the initial contaminated soil Cu^{2+} content of 398 mg/kg. The toxic leaching Cu^{2+} concentration of the soil in the S1 region was much lower than that in the other locations in the combined remediation, and the overall ion concentrations in the S2-S5 regions gradually decreased from cathode to anode. The main reason is that the copper ions in the soil migrate from the anode to the cathode and are enriched near the cathode. The S1 area is loaded with the solidifying agent, which can solidify a high concentration of copper ions. At this point, our group used a solidifying agent to remediate 6000 mg/kg high concentration contaminated kaolin with 99.9% remediation efficiency. When copper ions in the soil migrate to the area, they are fixed by the solidifying agent and trapped as well as being involved in the reaction. Due to the short remediation time, the chemical reaction in the solidifying agent is incomplete, so the Cu^{2+} concentration after the leaching toxicity test is approximately 20 mg/kg, which still meets all values lower than the leaching limit of 100 mg/L for Cu^{2+} specified in the Chinese standard[23]. If the remediation time is extended, the solidifying effect will improve[33]. Moreover, at the end of the experiment, the cathode electrolyte was also sampled for Cu^{2+} concentration, and the result was that almost no copper ions entered the cathode chamber, thus avoiding the disadvantage of secondary treatment of the electrolyte by the EK mediation technique. When the voltage intensity was 15 V, the copper ion content was higher in the S2-S5 regions than at the other voltage intensities, especially in the S2 and S4 regions. This may be due to the voltage, lower electric current, slower migration of copper ions, and low remediation efficiency due to the short remediation time. The remediation efficiencies were classified as 57.61%, 66.51%, 65.99%, and 68.01% after different voltage intensity (15 V, 30 V, 45

V, and 60 V) treatments.

The copper ion residues at each location after the completion of remediation in the control group are shown in Figure 10. Again, the copper ion content gradually increases from the anode to the cathode and is enriched in the region near the cathode (S1). This is because the copper ions combine with the OH^- generated in the cathode chamber during the migration to the cathode, forming a precipitate and enriching it. The higher concentration of copper ions in the S4 region may be due to the short remediation time, where Cu^{2+} migrates to the S4 region without having time to migrate to the cathode. Its remediation efficiency was 44.98%. Moreover, a large amount of black–green precipitate was observed in the electrolyte in the cathode chamber at the end of the test, which might be the generated $Cu(OH)_2$ precipitate. Excessive accumulation of precipitate would adhere to the electrode plate and affect the electrolysis reaction, which might be the reason for its low electric current.

In summary, the EK-S/S remediation technique is approximately 20% more efficient than the EK remediation technique, can overcome the aggregation effect and the disadvantages of secondary treatment of electrolytes in the EK remediation process, and can also bring together copper ions in one place for solidifying treatment, saving the disadvantages of disturbing the soil in a large area during the solidifying process. The solidifying agent is an environmentally friendly material that can be used for resource utilization of solid waste without causing harm to the environment and organisms. Therefore, this remediation technology is a proven means of enhanced electric remediation.

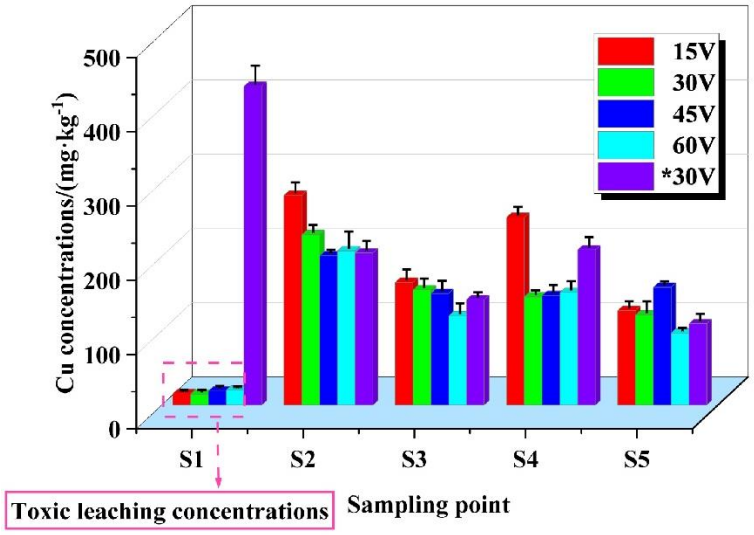

Figure 10. Cu^{2+} concentrations after remediation treatment at different locations under different voltage gradients.

3.6. Energy Analysis

The remediation efficiency and power consumption after combined EK-S/S and EK remediation treatments at different voltage gradients are shown in Table 3.

The results show that the higher the voltage is, the higher the electric current generated during the remediation process (Figure 1) is, resulting in higher electrical energy consumption. In the EK-S/S combined remediation test, the removal efficiency at a voltage of 30 V was approximately the same as that at voltages of 45 V and 60 V, but the electrical energy consumption was much lower than that at

voltages of 45 V and 60 V. Although it consumes more electrical energy than the 15 V and control groups, its remediation efficiency is much higher. Therefore, a constant voltage intensity of 30 V was chosen in this study, which has some advantages in terms of remediation efficiency and energy consumption. In subsequent studies, various enhancements, such as the addition of chelating agents, control of electrolyte pH, polarity exchange techniques, and variations in electrode materials and configurations, can be combined. Solar-powered technologies can also be combined to enhance the removal efficiency and reduce the energy consumption of copper ions from contaminated soil.

Table 3. Removal efficiency and power consumption

Number	Removal efficiency (%)	Power consumption (kWh/m^3)
15V	57.56	5.14
30V	66.51	14.62
45V	65.99	26.80
60V	68.01	39.96
*30V	44.98	4.84

3.7. Migration mechanism of anions and cations

Under the action of DC voltage, the migration patterns of anions and cations in soil are shown in Figure 11[34]. Specifically, an oxidation reaction occurs in the anode chamber, producing hydrogen ions (H^+), which move towards the cathode under a series of effects, such as ion migration, electrodialysis, and concentration diffusion, during which they continuously exchange ions with the cations in the soil contaminants (as shown in Equation 3). Moreover, the pore fluid in the soil chamber also moves towards the cathode under the effects of electrodialysis and diffusion, and the copper ions flow out of the soil on the way[35]. This combined remediation test is mainly to purify the soil by transporting copper ions to the S1 area near the cathode and using the solidifying agent to fix and trap the copper ions. This is similar to the approach of Ghobadi[36], where activated carbon and biochar were added mainly near the cathode area to immobilize the copper migrating to this location. Reduction reactions occur in the cathode chamber to produce hydroxide ions (OH^-), in addition to neutralization reactions (Equation 4), precipitation reactions (Equation 5), complexation reactions (Equation 6), and reduction reactions of copper ions (Equation 7) [37]. Among them, the precipitation reaction is the main reason for the aggregation effect in the electric remediation process[38]. The solids formed by the precipitation reaction will fill the pores in the soil and lead to the blockage of copper ion migration channels.

$$M^{n+}+nM^{+}\rightarrow nH^{+}+M^{n+} \quad (3)$$

$$H^{+}+OH^{-}\rightarrow H_2O \quad (4)$$

$$M^{n+}+n\ OH^{-}\rightarrow M(OH)_n\downarrow \quad (5)$$

$$M^{n+}+n\ OH^{-}\rightarrow M(OH)_m^{(n-m)+} \quad (6)$$

$$M^{n+}+ne^{-}\rightarrow M \quad (7)$$

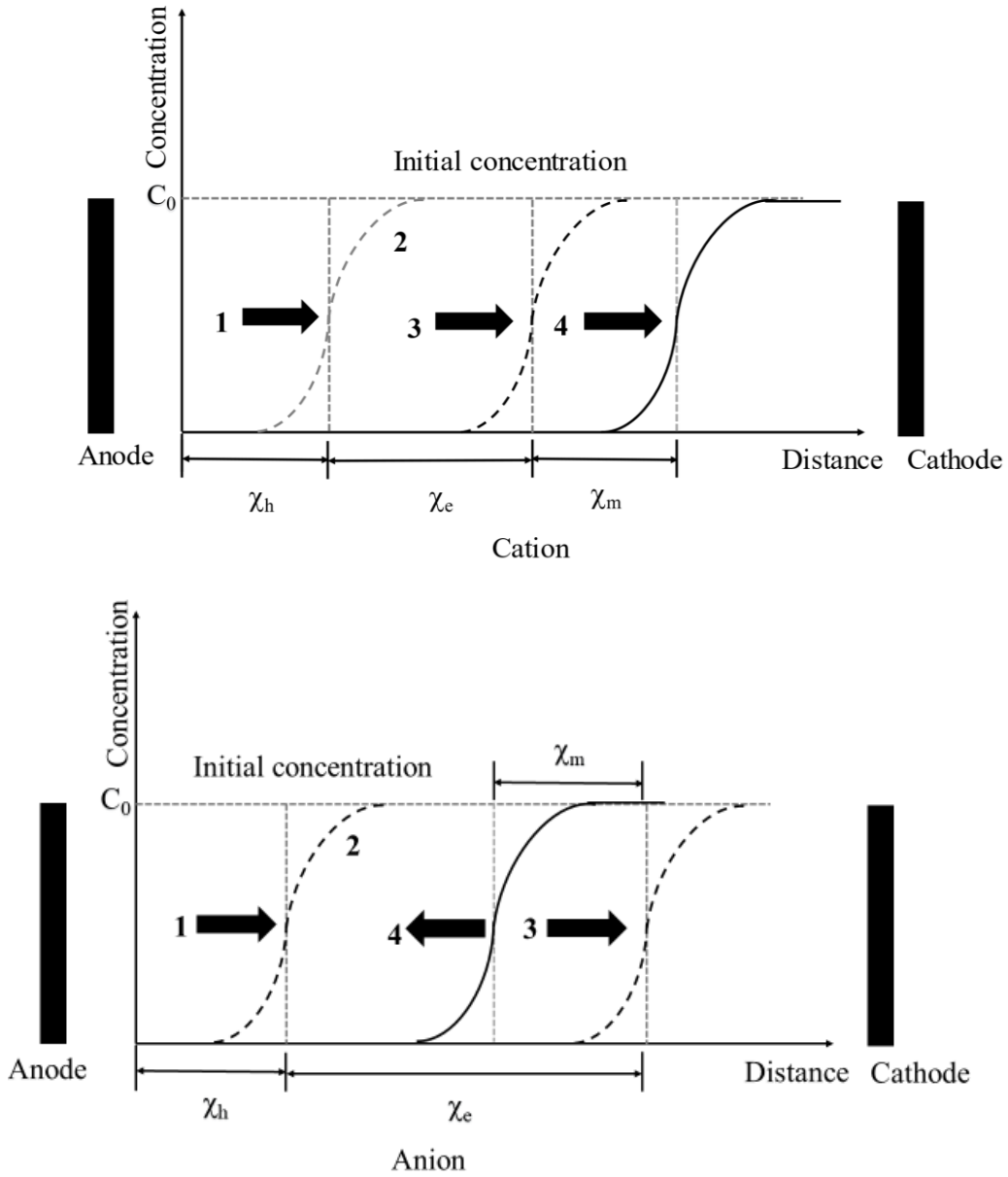

Figure 11. Migration mechanism of anions and cations: 1-Horizontal hydraulic pressure $X_h=(k_hi_h)T$, 2-Diffusion, 3-Electroosmotic flow $X_e=(k_ei_e)T$, 4-Ion migration $X_m=(ui_e)T$.

The EK-S/S combined remediation (30 V) and EK remediation (*30 V) in this experimental study were in sharp contrast to one another. The electric current of EK remediation reached a low value soon after a period of remediation and then always maintained a lower value. After remediation, copper ions were aggregated in the S1 and S4 regions, so the remediation efficiency was not high. In contrast, the combined remediation electric current decreases smoothly and always maintains a higher value afterwards, the copper ions are fixed in the S1 region, and the concentration of leaching toxic ions is smaller, so its remediation efficiency is higher. This is consistent with the improved electrokinetic removal of copper from contaminated soils by reactive filter media in the study[36], enhancing their remediation efficiency.

3.8. Solid waste solidification mechanisms

In this study, an HBSC-based solidifying agent RM:FA ratio of 8:2 was determined to be the optimal ratio, where FA and large amounts of both SiO_2 and Al_2O_3 can be used as raw materials for the hydration products. Additionally, the silica-aluminium gel formed by silica-oxygen tetrahedra SiO_4 and aluminium-oxygen tetrahedra AlO_4 in FA at the same time resulted in a more compact structure, which could trap and fix Cu^{2+} to reduce the migration rate of copper ions[39-41]. Note that the amount of RM used in this solidifying agent was large. Bayer RM mainly contains minerals, such as gibbsite, katoite, calcite, and cancrinite. Additionally, RM dissolved in water can be eliminated by anions such as OH^-, CO_3^{2-}, and $Al(OH)^{4-}$, as well as cations such as Al^{3+}, Ca^{2+}, and Na^+. The active material in RM participates in the hydration reaction to generate a gel material, thereby filling the pores and improving the strength of the solidifying body[42]. Solidifying agents with small amounts of cement, as well as HBSC containing large amounts of $CaSO_4$ and C_2S, may provide Ca^{2+} and SO_4^{2-} for the chemical reaction to promote the formation of AFt and other cementitious substances[43]. With the increase in curing time, AFt with a large specific surface area and certain expansion stress gradually interpenetrated with other hydration products in the form of microcrystals[44], reducing the pore space between soil mass grains and making the cured soil structure denser. This, in turn, increased the strength of the solidified body. In addition, Cu^{2+} in an alkaline environment forms $Cu(OH)_2$ precipitates[45,46], thereby reducing the content of Cu^{2+} in contaminated soil and decreasing the migration ability of Cu^{2+}, as shown in Figure 12. The addition of small amounts of cement was not only conducive to solidifying Cu^{2+} but also increased the strength of the solidifying body. In the hydration slurry, the needle and rod-like calcium alumina phase interspersed between the gel to form a calcium vanadium skeleton. The presence of large amounts of silica-alumina gel and other gels filled the middle of the skeleton so that the entire solidifying body formed a denser structure to improve the strength of the solidifying body.

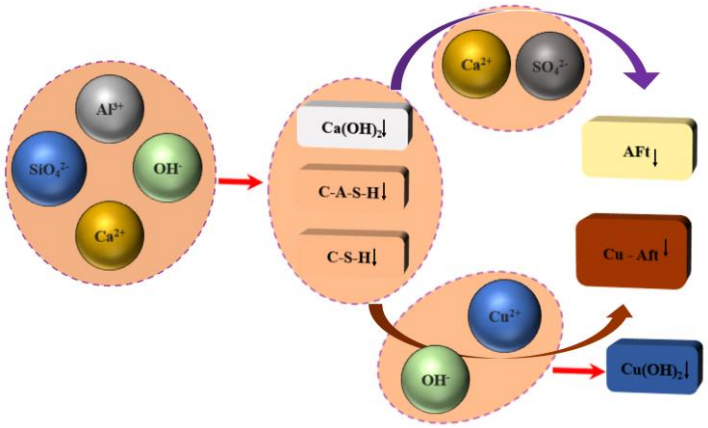

Figure 12. The solidification mechanism of the solidified body.

4. CONCLUSIONS

(1) The EK-S/S combined remediation technique had a remediation efficiency approximately 20%

higher than that of EK remediation alone, while avoiding the occurrence of the aggregation effect and enhancing the removal rate of Cu^{2+}.

(2) Two types of solid wastes, low-energy HBSC and a small amount of quicklime, were selected as solidifying agents, which not only achieved the resource utilization of solid wastes but also effectively solidified the copper ion that migrated to the area near the cathode during the remediation process. The ability of the solidifying agent to solidify copper ions will increase with increasing remediation time.

(3) During the remediation process, an oxidation reaction occurs at the anode, which reduces the anode electrolyte pH to between 1.5-2.2, and a reduction reaction occurs at the cathode, which reduces the anode electrolyte pH to 11 or less. This causes a change in the acid-base conditions of the soil in the soil chamber, in addition to a series of changes in EC, moisture contents, and copper ion residues.

(4) When 30 V was applied, the remediation efficiency of the combined remediation technology was 66.51%, which was 20% higher than the electric remediation efficiency, and the energy consumption was only 14.62 kWh/m^3. 30 V is a good choice as the voltage for the EK-S/S combined remediation process, both in terms of remediation efficiency and energy analysis.

ACKNOWLEDGEMENTS
This work was funded by National Natural Science Foundation of China (Grant No. 41807256, 51178287), Applied Basic Research Program in Shanxi Province (Grant No. 20210302123139), 2021 Key Projects of Innovation and Entrepreneurship Projects for College Students in Shanxi Province (Grant No. 202110112050).

References

1. Q. Yang, Z. Li, X. Lu, Q. Duan, L. Huang and J. Bi, *Sci. Total Environ.*, 642 (2018) 690.
2. Q. Duan, J. Lee, Y. Liu, H. Chen and H. Hu, *Bull. Environ. Contam. Toxicol.*, 97 (2016) 303.
3. M. Jaishankar, T. Tseten, N. Anbalagan, B. B. Mathew and K. N. Beeregowda, *Interdiscip. Toxicol.*, 7 (2014) 60.
4. K. Rehman, F Fatima, I Waheed, and M.S.H. Akash, *J. Cell. Biochem.*, 119 (2018) 157.
5. Y. Wu, X. Li, L. Yu, T. Wang, J. Wang and T. Liu, *Resour. Conserv. Recycl.*, 181 (2022) 106261.
6. A. Kumar, B. S. Bisht, V. D. Joshi and T. Dhewa, *Int. J. Environ. Sci. Technol.*, 1 (2011) 1079.
7. Y. Chen, D. Zhi, Y. Zhou, A. Huang, S. Wu, B. Yao, and C. Sun, *J. Ind. Eng. Chem.*, 97 (2021) 163.
8. S. Senevirathna, R. Mahinroosta, M. Li and K. KrishnaPillai, *Chemosphere*, 262 (2021) 127606.
9. T. Yang, Y. Xue, X. Liu and Z. Zhang, *Process Saf. Environ. Prot.*, 157 (2022) 509.
10. A. Reza, S. Anzum, R. C. Saha, S. Chakraborty and M. H. Rahman, *E3S Web of Conferences*, 96 (2019) 01003.
11. S. O. Ko, M. A. Schlautman and E. R. Carraway, *Environ. Sci. Technol.*, 33 (1999) 2765.
12. S. Yuan, Z. Zheng, J. Chen and X. Lu, *J. Hazard. Mater.*, 162 (2009) 1583.
13. E. K. Jeon, S. R. Ryu, K. Baek, *Electrochim. Acta*, 181 (2015) 160.
14. J. Virkutyte, M. Sillanpää, and P. Latostenmaa, *Sci. Total Environ.*, 289 (2002) 97.
15. Y. Wang, A. Li and C. Cui, *Chemosphere*, 265 (2021) 129071.
16. J. H. Choi, S. Maruthamuthu, H. G. Lee, T. H. Ha, J. H. Bae and A. N. Alshawabkeh, *J. Appl. Electrochem.*,40 (2010) 1101.
17. M. S. Torabi, G. Asadollahfardi, M. Rezaee and N. B. Panah, *J. Hazard. Toxic Radioact. Waste,* 25 (2021) 05020007.
18. L. Cang, Q. Y. Wang, D. M. Zhou, and H. Xu, *Sep. Purif. Technol.*, 79 (2011) 246.
19. L. Yuan, H. Li, X. Xu, J. Zhang, N. Wang and H. Yu, *Electrochim. Acta*, 213 (2016) 140.

20. L. Cang, D. M. Zhou, Q. Y. Wang and D. Y. Wu, *J. Hazard. Mater.*, 172 (2009) 1602.
21. T. Kimura, K. I. Takase and S. Tanaka, *J. Hazard. Mater.*, 143 (2007) 668.
22. H. Gao, Y. Yang, Q. Huang and Q. Wang, *J. Mater. Cycles Waste Manage.*, 19 (2017) 241.
23. H. Duan, Q. Huang, Q. Wang, B. Zhou and J Li, *J. Hazard. Mater.*, 158 (2008) 221.
24. T. R. Sun, L. M. Ottosen, P. E. Jensen and G. M. Kirkelund, *Electrochim. Acta*, 107 (2013) 187.
25. P. Drogui, J. F. Blais and G. Mercier, *Recent Pat. Eng.*, 1 (2007) 257.
26. M. T. Ammami, F. Portet-Koltalo, A. Benamar, C. Duclairoir-Poc, H. Wang and F. Le Derf, *Chemosphere*, 125 (2015) 1.
27. Y. B. Acar, A. N. Alshawabkeh, *Environ. Sci. Technol.*, 27 (1993) 2638.
28. A. Ayyanar, S. Thatikonda, *Soil Sediment Contam.*, 30 (2021) 12.
29. J. Virkutyte, M. Sillanpää and P. Latostenmaa, *Sci. Total Environ.*, 289 (2002) 97.
30. E. Gidarakos and A. Giannis, *Water Air Soil Pollut.*, 172 (2006) 295.
31. M. G. Nogueira, M.Pazos, M. A. Sanromán, and C. Cameselle, *Electrochim. Acta*, 52 (2007) 3349.
32. O. M. Boulakradeche, O. Merdoud and D. E. Akretche, *Environ. Eng. Res.*, 27 (2022).
33. C. Suo, P. Fang, H. Cao, J. Cao, K. Liu and X. Dong, *Constr. Build. Mater.*, 305 (2021) 124651.
34. O. A. Ahmed, Z. Derriche, M. Kameche, A. Bahmani, H. Souli, P. Dubujet and J. M. Fleureau, *Chem. Eng. Process. Process Intensif.*,100 (2016) 37.
35. D. Wen, R. Fu and Q Li, *J. Hazard. Mater.*, 401 (2021) 123345.
36. R. Ghobadi, A. Altaee, J. L. Zhou, P. McLean, and S. Yadav, *Chemosphere*, 252 (2020) 126607.
37. M. R. Gunsinger, C. J. Ptacek, D. W. Blowes, J. L. Jambor and M. C. Moncur, *Appl. Geochem.*, 21 (2006) 1301.
38. M. Vocciante, V. G. Dovì and S. Ferro, *Sustainability*, 13 (2021) 770.
39. D. Peng, Y. Wang, X. Liu, B. Tang and N. Zhang, *J. Hazard. Mater.*, 373 (2019) 294.
40. A. F. Bertocchi, M. Ghiani, R. Peretti and A. Zucca, *J. Hazard. Mater.*, 134 (2006) 112.
41. A. T. Lima, L. M. Ottosen and A. B. Ribeiro, *J. Environ. Manage.*, 95 (2012) S110.
42. Wang, Z., Wang, Y., Wu, L., Wu, A., Ruan, Z., Zhang, M., & R. Zhao, *Constr. Build Mater.*, 328 (2022) 127002.
43. Y. Zhang, P. Yu, F. Pan and Y. He, *Constr. Build. Mater.*, 190 (2018) 985.
44. M. Balonis and F. P. Glasser, *Cem. Concr. Res.*, 39 (2009) 733.
45. T. Wang, Y. Cao, G. Qu, Q. Sun, T. Xia, X. Guo and L. Zhu, *Environ. Sci. Technol.*,52 (2018) 7884.
46. Y. J. Sun, J. Ma, Y. G. Chen, B. H. Tan and W. J. Cheng, *Environ. Earth Sci.*, 79 (2020) 1.